

Electron Emission Yield Measurement of Polymers Induced by Electron and Photon

Jiang Wu^{1,2†}, Akira Miyahara¹, Kazuhiro Toyoda¹, Mengu Cho¹, Xiaoquan Zheng²

(1. *Kyushu Institute of Technology, Kitakyushu, Japan,*

2. *Xi'an Jiaotong University, Xi'an, China)*

† k300610u@tobata.isc.kyutech.ac.jp

Abstract— The surface potential of the spacecraft material depends on the current balance equation, in which the emitted electrons induced by the ambient plasma and solar photon bombardment play two main items. The spacecraft thermal protection materials polyimide and polyethylene terephthalate were chosen, and the total electron emission yield was measured by a small cylinder collector while the photoelectron emission yield by a vacuum ultraviolet lamp with 5 narrow band filters. Meanwhile, the pulse shot and sample scanning method were utilized in both systems to prevent surface charging phenomenon. According to the orbital environments, the comparison of total electron emission yield between virgin and ultraviolet irradiated samples was carried out, and the angular dependence of photoelectron emission yield was also tested and analyzed. The electron emission yield of various surface materials under different constraint conditions can establish the database, which will finally be used in the Multi-utility Spacecraft Charging Analysis Tool (MUSCAT) to accurately calculate the spacecraft surface potential.

Keywords— spacecraft surface dielectric; total electron emission yield; photoelectron emission yield; surface potential.

I. INTRODUCTION

ACCORDING to the current balance equation, the electron emission yield of the spacecraft surface materials plays the crucial role in spacecraft potential, especially the total electron emission yield (TEEY) and photoelectron emission yield (PEY) [1][2]. As the impact of fast moving electrons in the ambient plasma, the long term operation of spacecraft will gradually lead to the big potential difference on the surface boundaries because of different electron emission property. Usually the weakest part, the triple-junction (conductor, insulator and vacuum), will initiate discharge or even arcing phenomenon, which will damage the spacecraft seriously. Therefore, in order to take use of the MUSCAT for surface potential calculation, at least the database of the TEEY and PEY for various spacecraft surface materials is necessary.

However, the Low Earth Orbit (LEO) spacecraft is not only influenced by the orbital high density and low energy plasma, but also the solar ultraviolet irradiation and other degradation effects. The ultraviolet irradiation is accompanied with plenty of energetic photons which can activate the surface physical and chemical variation; also as the spacecraft is rotating in orbit, the electron emission yield will vary with the incident photon angles. For the

TEEY and PEY respectively, the above two factors will influence the yield, thus the charging property.

As the spacecraft thermal control material, the polyimide (PI) and polyethylene terephthalate (PET) film possesses high insulation and well thermal performance and are widely used in the spacecraft body and solar array. Based on the long-period developed TEEY and PEY measurement system, the TEEY of the virgin, ultraviolet irradiated PI and PET, and the PEY of normal and angular injection for virgin PI and PET were investigated. The UV irradiation system was used for 5 doses and 3 doses for PI and PET respectively; the 30° angel was chosen as the angular injection for PEY of both materials.

II. ELECTRON EMISSION YIELD DEFINITION

A. Total Electron Emission Yield

The total electron emission yield is defined as the number ratio of emitted electrons and injected electrons (primary electrons) with certain primary energy and angel. The curve of TEEY with respect to primary electron energy in normal injection situation is shown Fig. 1. The universal curves exist for all solid materials, the shape of which depends on the 4 key parameters, namely the first and second crossover energy, E_1 and E_2 , where the yield reaches unity, and the maximum value of the yield and its related primary energy, σ_{\max} and E_{\max} [3].

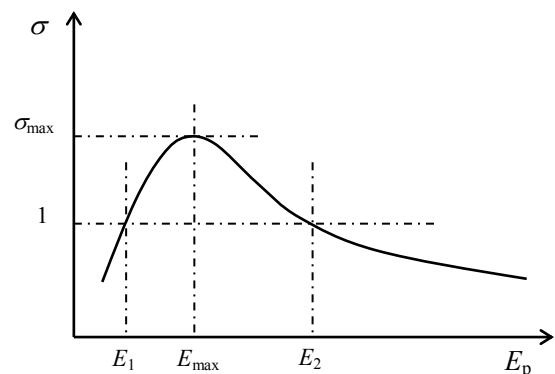


Fig. 1. Universal Curve of Total Electron Emission Yield for Solid Materials

B. Photoelectron Emission Yield

The photoelectron emission yield represents the number ratio of outgoing electron to the incident photon. The PEY varies with the incident photon energy or wavelength, the calculation equation expresses as follow [2].

$$\frac{I_{\text{photoelectron}}}{S} = q_e \cdot \int_0^{\infty} PF(\lambda) \cdot Y(\lambda) d\lambda \quad (1)$$

where $Y(\lambda)$ is the PEY of the certain material, $I_{\text{photoelectron}}$ is the photoelectron emission current, S is the light beam area, $PF(\lambda)$ is the photo flux, q_e is the unit charge.

III. EXPERIMENTAL PREPARATION

A. Total Electron Emission Yield System

The TEEY measurement system was developed on the base of JEOL JAMP-10 SXII Auger Microscope with a cylindrical metal collector. The chamber, with 7.0×10^{-5} Pa vacuum, is mounted the LaB₆ electron gun, which can emit the primary electron with energy ranging from 10eV to 10keV, 20nA current, 30 μ s pulse and 1mm² beam spot. The system can measure the TEEY of all solid plate samples with thickness less than 2.5mm. The system schematic is shown in Fig. 2. Comparing to the sample, the collector is biased to +50 V, in order to catch all the secondary electrons escaping from the sample surface [4][5].

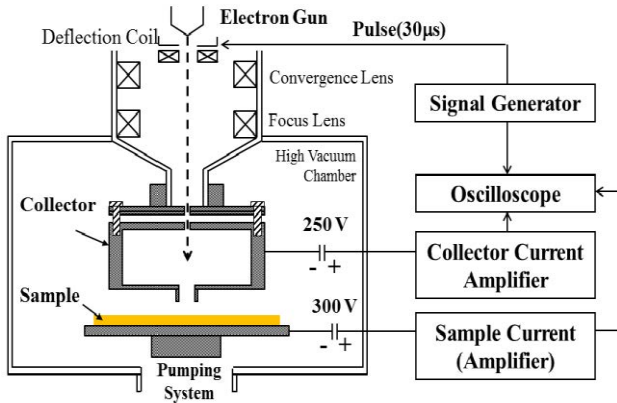


Fig. 2. Schematic of Total Electron Emission Yield System

In the TEEY system, when the primary electron hits the sample surface, the collector and sample current is measured simultaneously and then the yield σ can be calculated as follow.

$$\sigma = \frac{N_{\text{out_electron}}}{N_{\text{in_electron}}} = \frac{I_{\text{collector}}}{I_{\text{primary}}} = \frac{I_{\text{collector}}}{I_{\text{collector}} + I_{\text{sample}}} \quad (2)$$

To calibrate the measurement system, the TEEY of gold material was tested. The Fig. 3 shows the experimental results by red circles and comparison with reference data [6].

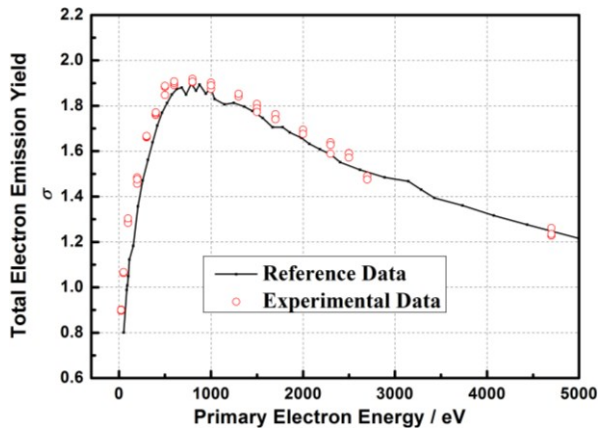


Fig. 3. TEEY System Calibration by Gold Material

B. Photoelectron Emission Yield System

The photoelectron emission yield system includes the

vacuum system, the compressor, the HAMAMATSU Inc.(Japan) Model L1835 Deuterium Lamp, with wavelength ranging from 115nm to 400nm, and the HAMAMATSU Inc. Model H8496-16 UV Laser Sensor with spectral response from 160nm to 220nm. The system schematic is depicted in Fig. 4, while Fig. 5 shows the relative intensity of the D2 lamp. The five narrow band filters were used for the incident photon, and their transmittance property was shown in Fig. 6. In the measurement system, the motor driven shutter is used to control the light pulse, with the pulse width around 200ms. The sample plate is grounded while the collector is biased to +15V for photoelectron receiving.

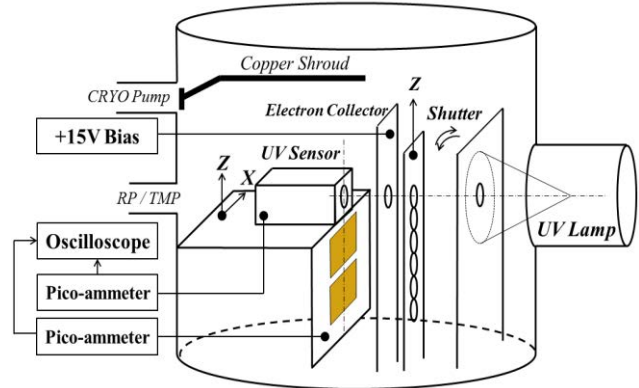


Fig. 4. Schematic of Photoelectron Emission Yield System

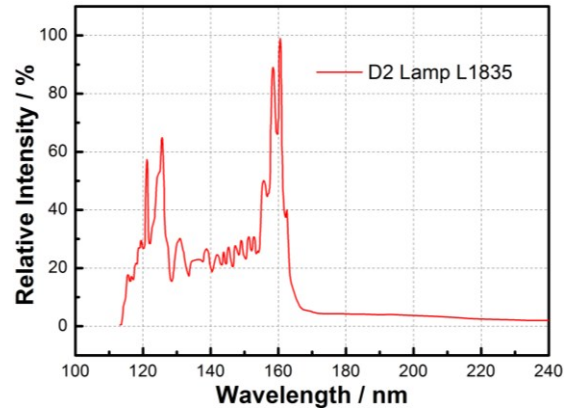


Fig. 5. Relative Intensity of D2 Lamp L1835

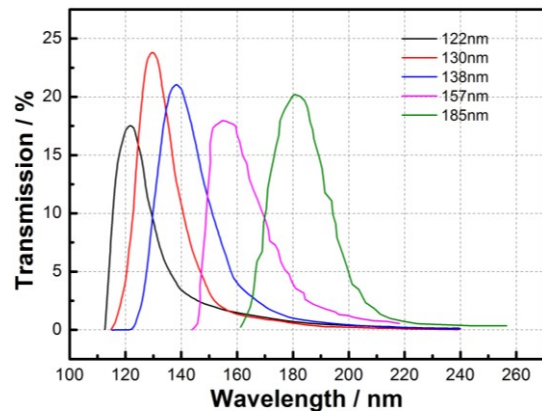


Fig. 6. Transmittance Property of Five Narrow Band Filters

As the UV light passes through the filters, the photo flux distribution will depend on the filter property. For calculating the photo flux acts on the sample, the filter property $NBF(\lambda)$ should be added to the right side of Equ. (1), then it turns to

$$\frac{I_{photoelectron_n}}{S} = q_e \cdot \int_0^\infty PF(\lambda) \cdot Y(\lambda) \cdot NBF_n(\lambda) d\lambda \quad (3)$$

where $n=1\sim5$, represents the five filter situations. In order to calculate the $Y(\lambda)$ in Equ. (3), we primarily assumed the linear function as:

$$Y(\lambda) = a \cdot \lambda + b \quad (4)$$

where a and b are the parameters. Taking Equ. (4) back to Equ. (3), we can obtain the five calculated photoelectron currents, which then are compared with the experimental photoelectron current under five different filter situations respectively. And the difference Δ between these two types of currents is defined as follow.

$$\Delta = \sum_{n=1}^5 \left(\frac{I_{calculated_n}}{I_{experimental_n}} - 1 \right)^2 \quad (5)$$

When the difference Δ reaches minimum, then the best value for a and b is obtained, also the PEY property.

Based on this simulation method, we measured the gold material to calibrate the system as shown in Fig. 7. The calculated photoelectron current from simulated PEY and experimental photoelectron current is also compared in Fig. 7 [8].

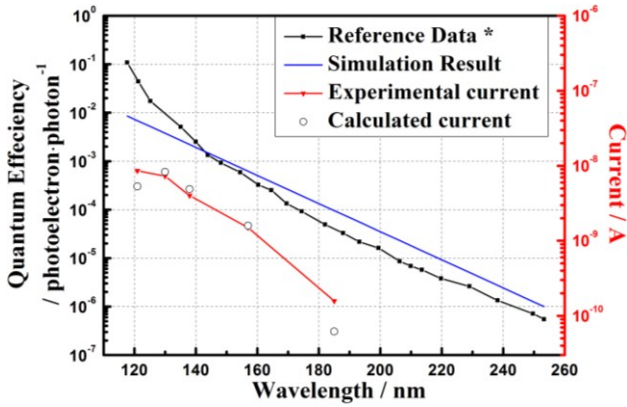


Fig. 7. PEY System Calibration by Gold Material

C. Sample Pretreatment

The TOREN DuPont Inc.(Japan) manufactured Kapton 100H type polyimide with 25 μ m thickness, and PET film with 50 μ m were chosen as research objects. The film was cut to be 35mm \times 35mm square shape, and ultrasonically cleaned by alcohol in advance. Before the TEEY or PEY testing, the backside of the samples were coated with Au as the electrode by the SANYU Electronics Inc.(Japan) QC-701 type Quick Coater, and electric potential of the testing side was checked by the TREK Inc.(USA) 362A type Electrostatic Voltmeter. If the potential is higher than $\pm 5V$, the Omron Inc.(Japan) ZJ-FA20 type Ionizer was used to neutralize the surface and eliminate the effect of charging.

D. Solutions for Surface Charging

In the case of insulation material, the surface charging will influence the electron emission yield, as the generated electron will be trapped by the surface potential. In order to solve this problem, two solutions are proposed for both systems. Firstly, during the measurement the sample moves step by step, and Fig. 8 illustrates the measuring positions on sample, and each position is only measured for one electron or photon shot. Secondly, we used the pulse control for each electron or photon shot. The pulse width is 30 μ s and 200ms for TEEY and PEY system respectively.

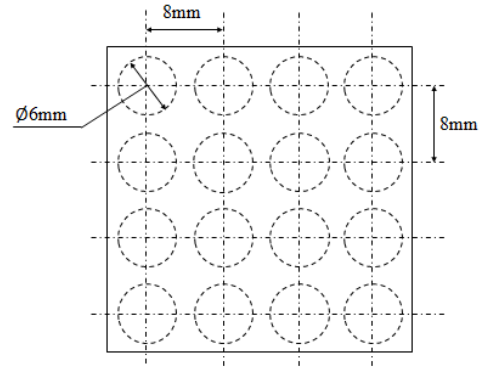


Fig. 8. Measurement Position on Sample for Scanning Method

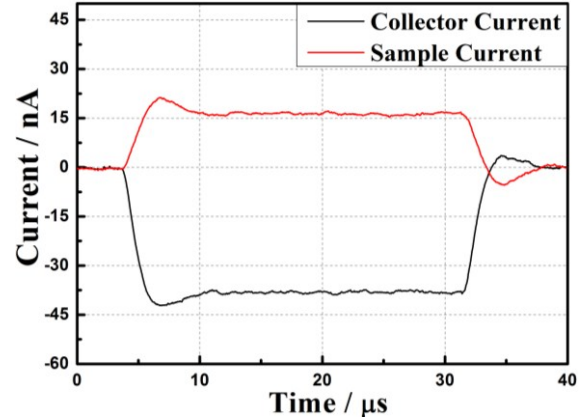


Fig. 9 TEEY Current Waveform of Polyimide at 150eV

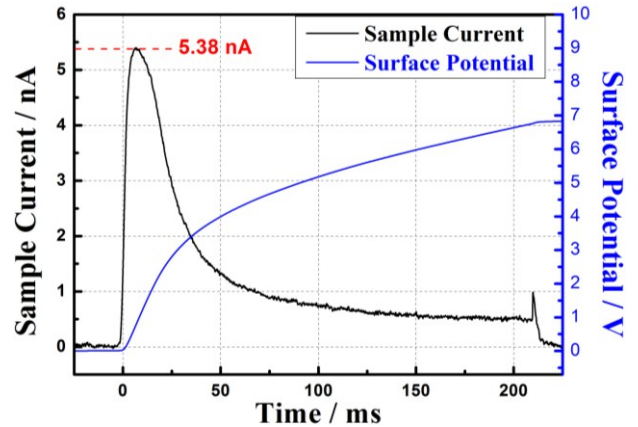


Fig. 10. PEY Current Waveform of Polyimide at 122nm Filter Situation

Fig. 9 and 10 show the typical current waveform of the TEEY and PEY of polyimide respectively. From Fig. 9, the current waveform's flatness proves that the surface charging is not obvious; while for PEY measurement current wavelength of polyimide shown in Fig. 10, the surface charging occurred and the surface potential is around +7V. However, as the collector in PEY system is biased to +15V, we consider that the photoelectron can still escape from the sample surface.

E. Ultraviolet Irradiation System

The UV irradiation system includes vacuum and low temperature, optical, sample moving and some auxiliary parts. The UV lamp is HAMAMATSU Inc.(Japan) Model L1835 Deuterium Lamp, with wavelength ranging from 115nm to 400nm and intensity is 2.23mW/cm², and the UV Laser Sensor is HAMAMATSU Inc. Model H8496-16 with spectral response from 160nm to 220nm. The irradiation

situation was as follow: 8.0×10^{-5} Pa chamber vacuum, -150°C copper shroud and 28°C sample temperature during irradiation. The PC program drove the system and the UV irradiation intensity distribution of sample position was automatically checked by the UV sensor every 30min. After UV irradiation, the sample was directly installed on the sample plate and together inserted into the TEEY chamber, with not more than 10min air exposure.

IV. EXPERIMENTAL RESULTS

A. Total Electron Emission Yield

a. Virgin PI and PET Film

The TEEY of pretreated PI and PET film was measured in room temperature. Due to the material dispersion, several groups of virgin PI and PET data were averaged as the result, shown in Fig. 11(a). Tab. I shows the key parameters for the TEEY property of polyimide film.

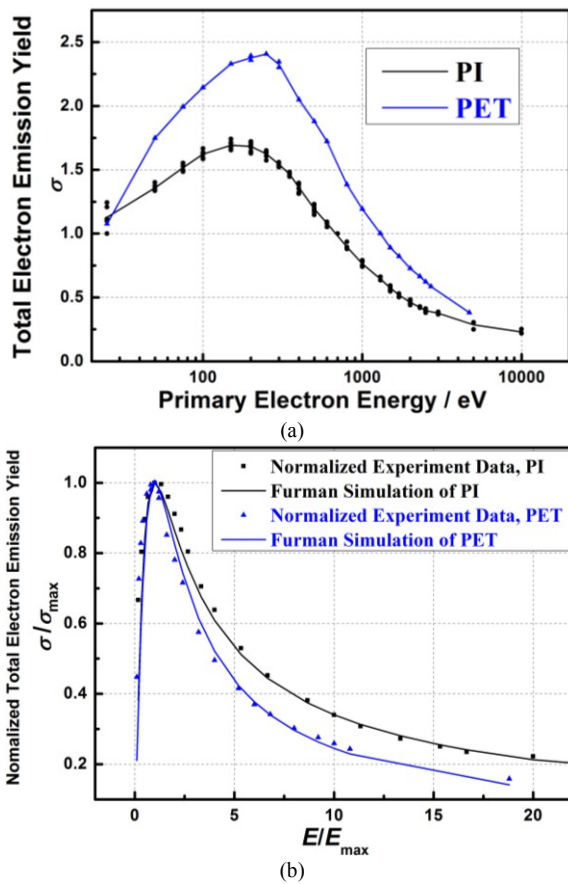


Fig. 11 Total Electron Emission Yield of Virgin PI and PET
(a) Experimental Data (b) Comparison with Furman Simulation

Tab. I Parameters for TEEY of virgin PI and PET Film

| Items | PI | PET |
|-----------------|--------------|-----------|
| E_1 | ~ 25 eV | < 25 eV |
| E_2 | 650 eV | 1300 eV |
| E_{\max} | 150 eV | 250 eV |
| σ_{\max} | 1.7 | 2.4 |

According to the simulation theory of secondary electron emission yield (SEEY) by Furman, the relationship between the electron yield and primary electron energy follows as [7]

$$\delta(E_p) = \delta_{\max} \cdot \frac{s \cdot (E_p / E_{\max})}{s - 1 + (E_p / E_{\max})^2} \quad (6)$$

where the E_p is the primary electron energy, δ_{\max} is the maximum value of SEEY, E_{\max} is the primary electron energy when the δ_{\max} is reached, and s is the related coefficient ranging from 1 to 2 for solid material. As the SEEY dominates the TEEY, the simulation tendency should be same.

From Fig. 11(b) we can know that the tendency of the experimental data well matched with the Furman simulation data for both materials.

b. UV Degraded PI and PET Film

In this research, we chose 5 UV doses, including 17, 34, 100, 500 and 2000 equivalent solar hours (ESH) for PI film and 3 doses, including 100, 500, 1000 ESH for PET film. The TEEY results of virgin and UV degraded samples were shown in Fig. 12.

After UV degradation, the TEEY of PI gradually increased with doses rising, while finally saturated at 500 ESH; the TEEY of PET decreased with UV doses rising, and at 100 ESH it almost reached the minimum yield. Meanwhile, the E_{\max} for both materials maintained.

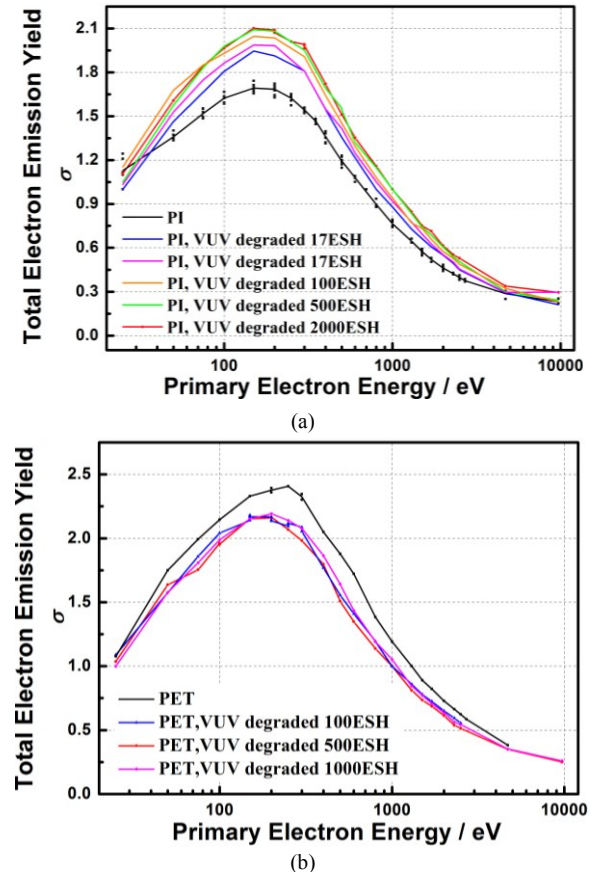


Fig. 12 Total Electron Emission Yield of UV Degraded PI and PET
(a) PI (b) PET

B. Photoelectron Emission Yield

a. Normal Injection for PI and PET Film

The PEY tests of virgin PI and PET were conducted in this research. Using the linear simulation method in Section III, we calculated the PEY property based on the experimental results. Fig. 13 (a) and (b) shows the PEY of both materials and the current comparison [8].

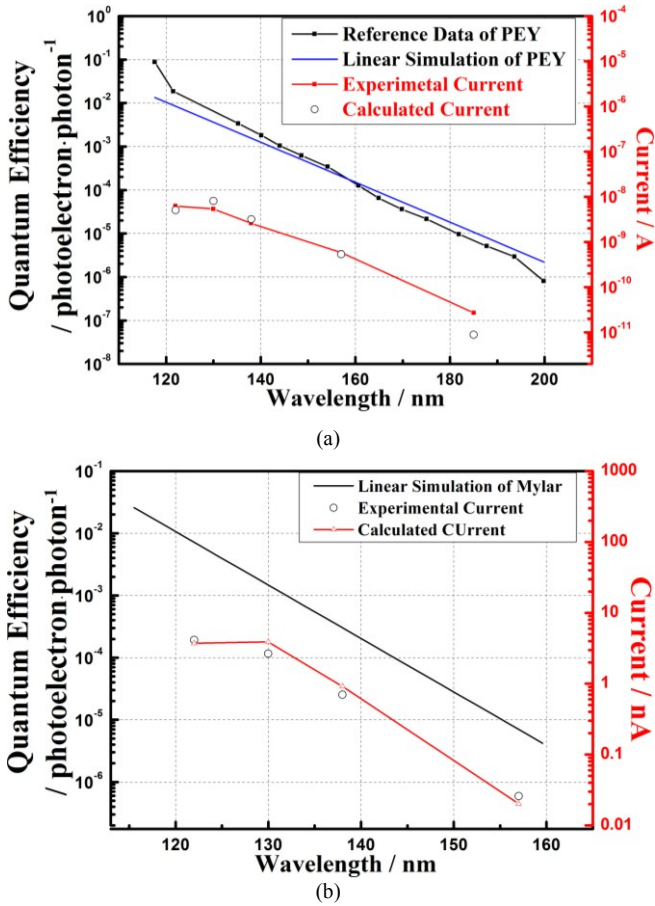


Fig. 13. Photoelectron Emission Yield of Virgin PI and PET at Normal Injection (a)PI (b)PET

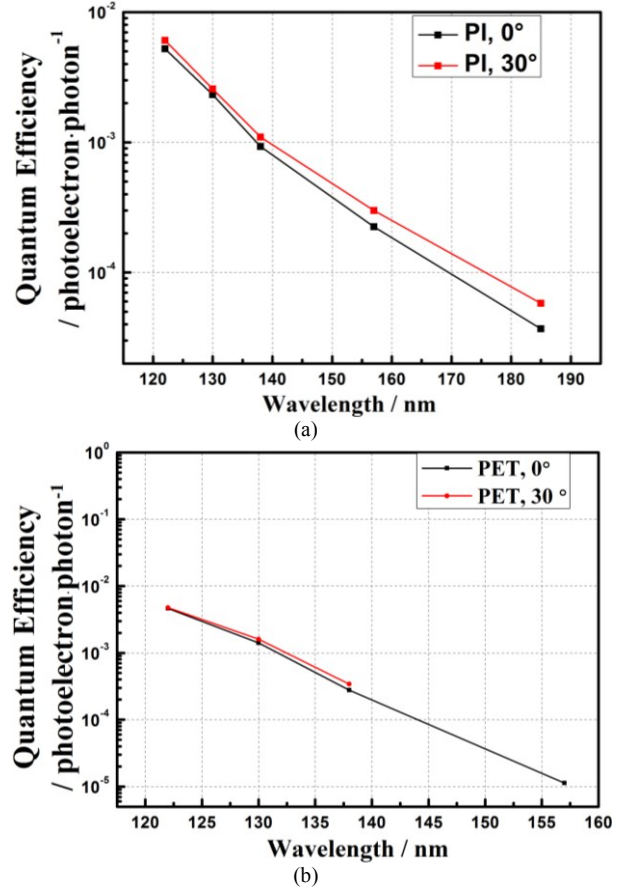


Fig. 14. Photoelectron Emission Yield of Virgin PI and PET at 30° Angle Injection (a)PI (b)PET

b. Angular Injection for PI and PET Film

The 30° angular injection PEY for both materials was also tested. Due to the system light beam is fixed, the sample plate was rotated for 30°. Fig. 14 (a) and (b) shows the experimental results for both materials.

Fig. 14 (a) and (b) infer that, when the injection angle rises, the PEY slightly increases for both materials.

V. ANALYSIS AND DISCUSSION

The electron emission yield induced by electron and photon for solid materials can be measured by our TEEY and PEY system.

For the TEEY of UV degraded materials, as the energetic photons acting on the material during UV irradiation may change the molecular structure of the polymer, and the total electron emission yield has deep relationship with surface chemical and physics status, thus it varies after UV irradiation. For further explanation, the XPS analysis is needed for the elements variation.

For the PEY simulation, in order to verify the accuracy of our simulation method, we calculated the photoelectron current density in D2 lamp full wavelength range by using the simulated PEY results, and compared with experimental data in the situation of no filter, as shown in Tab. II. For the gold material, the calculated currents density for both light sources are little smaller than the experimental data, which may result from the inaccuracy of simple linear simulation. Fig. 7 implied that, the PEY of gold material at short wavelength range is less than the reference data, and especially the PEY in this range is tens of thousand times of that in the long wavelength, so it plays an important roll for

calculating the photoelectron current. Therefore, the high order of nonlinear simulation is necessary to be used for accurate simulation in the future work. For polymers in Tab. II, the experimental current density is relatively smaller, which may be caused by surface charging, as shown in Fig. 10. In fact, the current waveform peak for full range D2 Lamp is even sharper than that of filter used situation in Fig. 10. In that case, the real current peak value hasn't appeared, but the waveform already begins to decay as the surface potential trapping the photoelectrons. So, the experimental current becomes smaller. So the shorter pulse is needed to improve the current measurement.

After we get the PEY simulation results, the photoelectron current density in space environment can also be calculated by using the AM0 solar distribution and compared with the real data from reference in Tab. II [2].

Tab. II. Current Comparison of Experimental and Simulated Data

| Material | Light Source | Calculated | Experimental |
|----------|--------------|---|---|
| | | Current Density / A·cm ⁻² | Current Density / A·cm ⁻² |
| Gold | D2 Lamp | 3.73×10 ⁻⁷ | 6.26×10 ⁻⁷ |
| | AM0 | 6.77×10 ⁻¹⁰ | 3.90×10 ⁻⁹ |
| PI | D2 Lamp | 3.17×10 ⁻⁷ | 2.51×10 ⁻⁷ |
| | AM0 | 3.71×10 ⁻¹⁰ | / |
| PET | D2 Lamp | 3.18×10 ⁻⁷ | 7.08×10 ⁻⁸ |
| | AM0 | 3.10×10 ⁻¹⁰ | / |

For the angular dependence of PEY, it is considered that the angular injection of photon leads to the different light reflectance for the materials, which changes the photon absorption and finally the PEY. Thus, the optical analysis will be carried out to explain this result soon.

The analytical tests are needed for explain the entire experimental phenomenon. We also will conduct other degradation test such as atomic oxygen erosion, energetic electron and proton irradiation for the polymers, and investigate these degradation effects on total electron emission yield and photoelectron emission yield.

VI. CONCLUSION

- (1) Electron emission yield induced by electron and photon can be well measured, especially the insulation materials.
- (2) Comparing to the virgin material, the total electron emission yield of UV degraded PI film increases with rising UV dose while that of PET films decreases. The E_{\max} maintains for both degraded materials.
- (3) The 30° incident angle PEY of both PI and PET film slightly increases to the normal injection situation.

REFERENCE

- [1] S. T. Lai, *Fundamentals of Spacecraft Charging: Spacecraft Interactions with Space Plasmas*, Princeton University Press, 2011.
- [2] D. Hastings et al, *Space Environment Interaction*, Cambridge: Cambridge University Press, 1996.
- [3] G. F. Dionne, "Origin of secondary-electron-emission yield-curve parameters," *J. Appl. Phys.*, vol. 46, no. 8, pp. 3347-3351, 1975.
- [4] Y. Chen et al, "Total electron emission yield measurement of insulator by a scanning small detector," *Appl. Phys. Lett.*, vol. 99, p. 152101, 2011.
- [5] Y. Chen et al, "Photoelectron emission yield measurement of insulator by vacuum ultraviolet light source and several narrow bandwidth filters", presented at 12th Spacecraft Charging Technology Conference, Kitakyushu, Japan, May 13-18, 2012.
- [6] J. R. Dennison et al, "Evolution of the electron yield curves of insulators as a function of impinging electron fluence and energy," *IEEE Trans. Plasma Sci.*, vol. 34, no. 5, pp. 2204-2218, 2006.
- [7] M. A. Furman et al, "Probabilistic model for the simulation of secondary electron emission," *Phys. Rev. ST Accel. Beams*, 5, p.124404, 2002.
- [8] K. Nomura et al, "Measurement system of the development of the photoelectron emission on the spacecraft materials", presented at 12th Spacecraft Charging Technology Conference, Kitakyushu, Japan, May 13-18, 2012.
- [9] B. Feuerbacher et al, "Experimental investigation of photoemission from satellite surface materials", *J. Appl. Phys.*, vol. 43, no.4, 1972.